processes

MDPI

Article

Oscillation Times in Water Hammer Signatures: New Insights for the Evaluation of Diversion Effectiveness in Field Cases

Bingxiao Liu [1,2], Wenhan Yue [3], Yajing Wang [4], Zhibin Gu [1,2], Ran Wen [1], Yang Qiu [4], Pukang Yi [4] and Xiaodong Hu [4,*]

[1] Sichuan Changning Natural Gas Development Co., Ltd., Yibin 644005, China
[2] Sichuan Gemflower Xinsheng Oil and Gas Operation Service Co., Ltd., Chengdu 610051, China
[3] Shale Gas Research Institute of PetroChina Southwest Oil and Gas Field Branch, Chengdu 610051, China
[4] State Key Laboratory of Petroleum Resources and Engineering, China University of Petroleum, Beijing 102249, China
* Correspondence: huxiaodong@cup.edu.cn

Abstract: Diversion is a crucial technique for effectively improving shale reservoir production by creating more complex fracture networks. Evaluating diversion effectiveness is necessary to optimize the parameters in hydraulic fracturing. Water hammer diagnostics, an emerging fracturing diagnosis technique, evaluate diversion effectiveness by analyzing water hammer signals. The water hammer attenuation, as indicated by the oscillation time, correlates with the complexity of fracture networks. However, it remains unclear whether the oscillation time is associated with diversion effectiveness. This paper elucidates the relationship between the water hammer oscillation time and diversion effectiveness by taking the probability of diversion and the treating pressure response as the evaluation criteria. Initially, a high-frequency pressure sensor was installed at the wellhead to sample the water hammer signals. Next, the oscillation times were determined using the feature extraction method. Simultaneously, the probability of diversion and the treating pressure response were calculated using the cepstrum error function and treating pressure curve, respectively. Then, the relationship between the oscillation time and diversion effectiveness was analyzed. Finally, a rapid judgment method for evaluating diversion effectiveness based on the water hammer oscillation time was proposed. The results indicated a negative correlation between the probability of diversion and the oscillation time, with higher probabilities resulting in lower oscillation times. The oscillation times exhibited a negative correlation with the treating pressure response, including the treating pressure increases and diversion pressure spikes, wherein a greater pressure differential led to lower oscillation times. Drawing from the statistics of a shale gas horizontal well in Sichuan, a better diversion effectiveness is associated with fewer oscillations, demonstrating a negative correlation between the diversion effectiveness and the oscillation time in water hammer signatures. Finally, a rapid judgment method for evaluating diversion effectiveness was proposed, utilizing the 95% confidence interval of the mean oscillation time. This paper offers useful insights into evaluating diversion performance in field cases.

Keywords: hydraulic fracturing; water hammer diagnosis; diversion effectiveness; oscillation times; quefrency analysis; treating pressure analysis

check for updates

Citation: Liu, B.; Yue, W.; Wang, Y.; Gu, Z.; Wen, R.; Qiu, Y.; Yi, P.; Hu, X. Oscillation Times in Water Hammer Signatures: New Insights for the Evaluation of Diversion Effectiveness in Field Cases. *Processes* **2024**, *12*, 1312. https://doi.org/10.3390/pr12071312

Academic Editor: Chuanliang Yan

Received: 23 April 2024
Revised: 12 June 2024
Accepted: 14 June 2024
Published: 24 June 2024

Copyright: © 2024 by the authors. Licensee MDPI, Basel, Switzerland. This article is an open access article distributed under the terms and conditions of the Creative Commons Attribution (CC BY) license (https://creativecommons.org/licenses/by/4.0/).

1. Introduction

Diversion is a significant hydraulic fracturing technique widely applied in the field [1–4]. Effective diversion can facilitate the formation of a more complex fracture network within the shale reservoir, thereby significantly enhancing oil and gas production [5]. Evaluating the diversion effectiveness is the foundation of optimizing fracturing parameters, ensuring an efficient and cost-effective reservoir reconstruction [6,7]. Therefore, evaluating diversion effectiveness is necessary in field applications.

The treating pressure response, encompassing treating pressure increases and diversion pressure spikes, is the main method to diversion effectiveness by identifying the sudden pressure increases or specific pressure features [4,8,9]. The treating pressure varies with the extension and complexity of fractures. If the diverters perform effectively, the flow resistance increases, resulting in a significant rise in the treating pressure. Water hammer fracture diagnostics [10], an emerging technique for fracturing diagnosis, evaluate the diversion effectiveness using the cepstrum analysis and error function of water hammer signals [11]. Water hammer, a sudden pressure pulsation occurring upon pump shutdown, propagates along the wellbore and interacts with fractures or other downhole events [12–14]. These interactions alter the pressure signal feature, conveying valuable subsurface information that can be identified using water hammer diagnostics [3,15–17]. The attenuation of the water hammer signal is an important feature to reflect the complexity of fractures, while the water hammer oscillation time is an intuitive manifestation of attenuation. Ciezobka [18] proposed a concept concerning water hammer decay, focusing on the energy absorbed by the fracture network when the pressure pulse passed through it. A larger fracture network size would result in a higher water hammer decay. Iriarte [19] suggested that a higher decay rate was associated with increased production. The authors pointed out that additional fractures or a larger fracture network would make the water hammer decay faster. Hu [20] considered a strong correlation between the decay rate of the water hammer and the fracture numbers. The formation of more fractures was associated with the higher decay rate of the water hammer [20,21]. The correlation between water hammer decay and the scale of the fracture network was demonstrated in the research conducted by the aforementioned scholars. In field applications, water hammer diagnosis is extensively utilized for evaluating diversion effectiveness [3,4,16,22–26]. Nevertheless, it remains unclear whether the oscillation time is associated with diversion effectiveness.

In this paper, we carried out an on-site test of diversion in Sichuan, China. First of all, a high-frequency pressure sensor was installed at the wellhead to sample water hammer signals. Second, the feature extraction method for water hammer oscillation times was used to quantify the oscillation times within the field-sampled signal. Simultaneously, the probability of diversion and the treating pressure response were calculated using the cepstrum analysis and error function and treating pressure curve analysis, respectively. Then, the relationship between the oscillation time and diversion effectiveness in fracturing was analyzed. Finally, a rapid judgment method for evaluating diversion effectiveness based on the water hammer oscillation times was proposed. This study offers useful insights into evaluating diversion effectiveness, thereby laying the groundwork for optimizing fracturing parameters.

2. Methods

Water hammer fracture diagnosis is an easy-operation, economical, and real-time method for fracturing diagnosis. The water hammer wave is generated under the inertia. When the pumping fluid is stopped quickly, the sudden change in the flow rate causes water hammer pressure pulsation in the wellbore. The water hammer wave propagates along the wellbore, reflecting and carrying the downhole event information back to the wellhead when it encounters downhole events. A high-frequency sensor is installed at the wellbore to record the water hammer signal [27]. The sample rate is 1000 Hz, and the monitoring is carried out throughout the diversion. The configuration, including the high-frequency pressure sensor, data acquisition, and analysis system, is shown in Figure 1.

In this paper, the feature extraction of water hammer oscillation times was used to obtain the oscillation times, the cepstrum analysis and error function were used to calculate the probability of diversion, and the treating pressure response was used to obtain the treating pressure increase and diversion pressure spike.

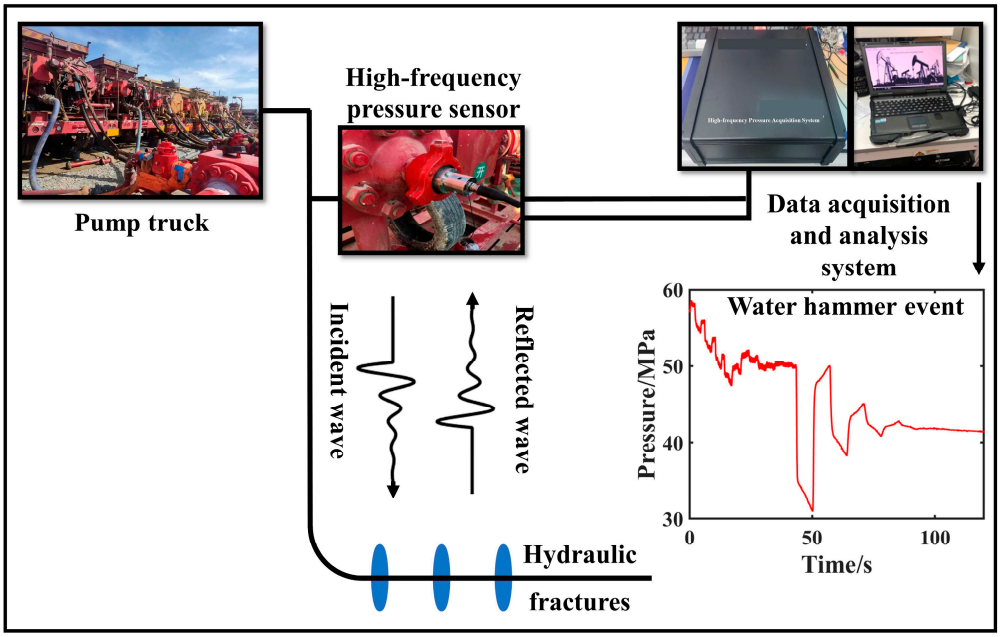


Figure 1. The equipment configuration. A pump truck is used to inject fracturing fluid. The water hammer will be generated when the pump track shuts down. The high-frequency sensor is installed at the wellhead to record the water hammer signal. The data acquisition and analysis system is used to process and analyze the sampled signals.

2.1. The Feature Extraction of Water Hammer Oscillation Times

The feature extraction method for water hammer oscillation times described in this paper is as follows (shown in Figure 2): first, the water hammer signal is intercepted from 30 s before pump shutdown to the end of acquisition. Second, a lowpass filter is used for the intercepted signal to ensure a clear waveform. Third, mean normalization is used to eliminate the influence of the absolute treating pressure on the oscillation times, making a consistent criterion at each stage.

$$P' = \frac{P - P_{min}}{P_{max} - P_{min}} \tag{1}$$

Here, P is the original water hammer signal (MPa), and P' is the processed signal by mean normalization (zero dimension). The processed signal P' is shown in Figure 3. The period is denoted as the duration between the two peaks of the water hammer signal. The period (*Period*, s) represents the time required for the water hammer wave to complete a round trip in the wellbore, which is defined as one water hammer oscillation.

$$Period = T_{P_2} - T_{P_1} \tag{2}$$

Here, T_{P_2} and T_{P_1} (s) represent the times corresponding to the two peaks. The peak-to-peak value (V_{pp}, zero dimension) is the pressure difference between the peak and the valley.

$$V_{PP} = P'_{max} - P'_{min} \tag{3}$$

When the normalized peak-to-peak value is less than 0.025, it is considered that there is no water hammer oscillation.

$$V_{PP} < 0.025 \tag{4}$$

This feature extraction method for water hammer oscillation times ensures a consistent criterion for counting the oscillation times at each stage.

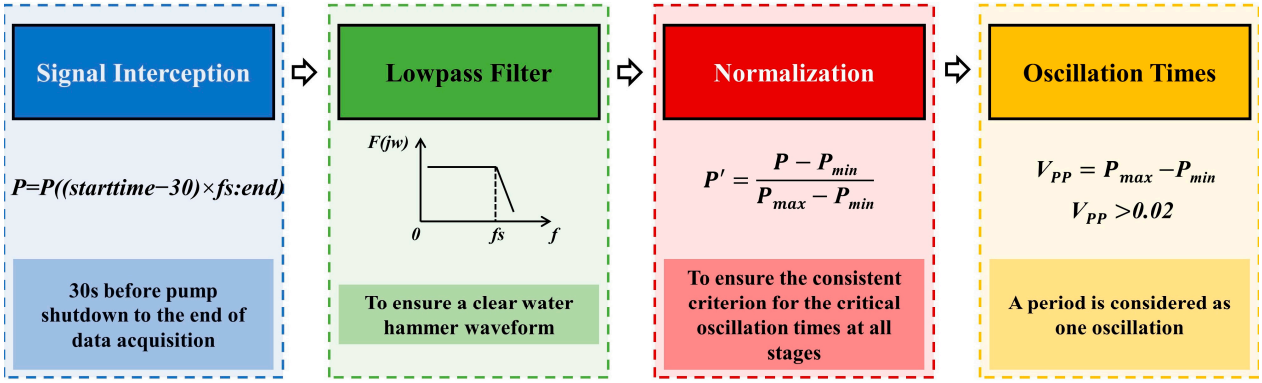


Figure 2. The feature extraction procedure of the water hammer oscillation times.

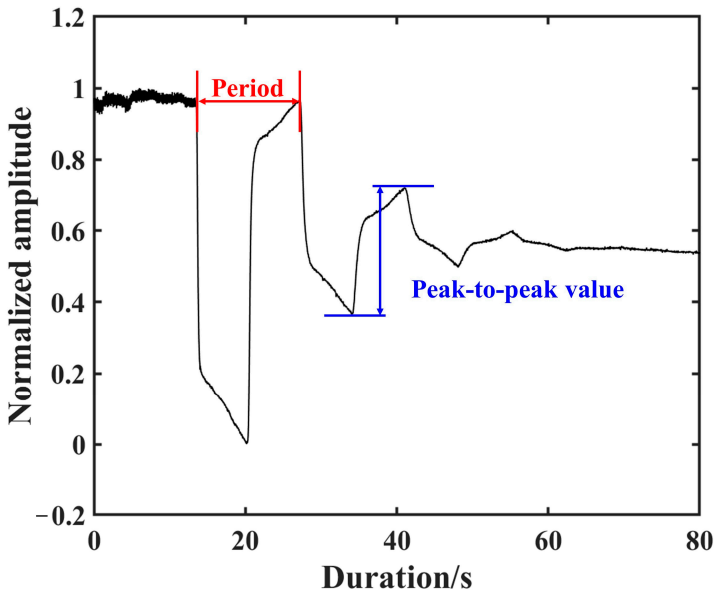


Figure 3. The processed water hammer signal and schematic diagram of oscillation times, including the defined period and peak-to-peak value.

2.2. The Cepstrum Analysis and Error Function

The cepstrum analysis is employed to analyze the diversion of the fluid acceptance zone, facilitating the evaluation of diversion effectiveness [15].

The calculation formula for the cepstrum analysis is as follows:

$$\hat{x}(\tau) = \frac{1}{2\pi} \int \log\left[\left|\int x(t)e^{jwt}dt\right|\right] e^{-jwt}dw \quad (5)$$

where τ is quefrency, with the characteristics of reflection time dimension; $x(t)$ and $\hat{x}(\tau)$ represent the signals in the time and quefrency domains. The water hammer signal was segmented into finite-length windows, and the cepstrum analysis was conducted. Integrating the cepstrum results of all windows, the cepstrogram of the water hammer was calculated. The cepstrogram serves as a visual representation of the water hammer cepstrum matrix (see Figure 4). The strong negative peak shown in Figure 4 is considered to be the downhole event response.

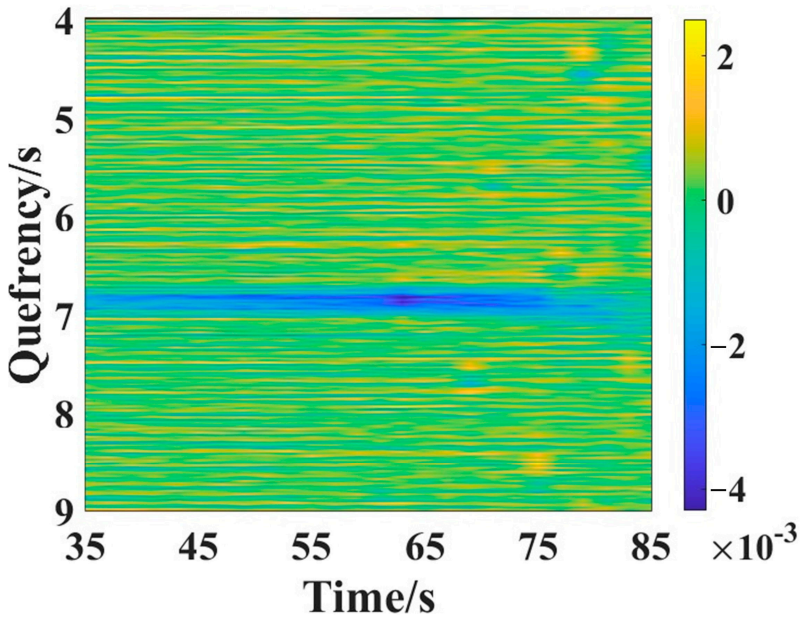


Figure 4. The cepstrum of the water hammer signal.

The following function was generated by taking the scalar product of vectors with different physical times (t_i and t_j):

$$F_{ij\tau} = V_{t_i,\tau} V_{t_j,\tau} \tag{6}$$

where i, j corresponds to two different points at different physical times, and τ denotes a centroid of each vector in the reflection time domain. By summing all vectors with a different physical time, the function F_τ, representing the reflection time, would be generated:

$$F_\tau = \sum_{ij} F_{ij} = \sum_{ij} V_{t_i} \cdot V_{t_j} \tag{7}$$

The quefrency τ of the peaks in F_τ denotes the reflection time of downhole events. The reflection location is calculated by:

$$L = \frac{a \times \tau}{2} \tag{8}$$

where L is the location of the reflection event (m), a is the wave speed in the pipeline, and τ is the time when the pressure trend is changed. For the events before and during diversion with depths L_1, L_2 and errors σ_1, σ_2, we can calculate the probability of diversion using the error function (Erf), described as follows:

$$prob = Erf\left(\frac{|L_2 - L_1|}{\sqrt{2({\sigma_1}^2 + {\sigma_2}^2)}}\right) \times 100\% \tag{9}$$

For example, for the events "Diversion" and "Shutdown" (see Figure 5), L_1 = 4903 m, L_2 = 4943 m, σ_1 = 46 m, and σ_2 = 37 m. The calculation of the probability of diversion based on depths and errors suggests that the diversion probability between "Diversion" and "Shutdown" is 97.83%.

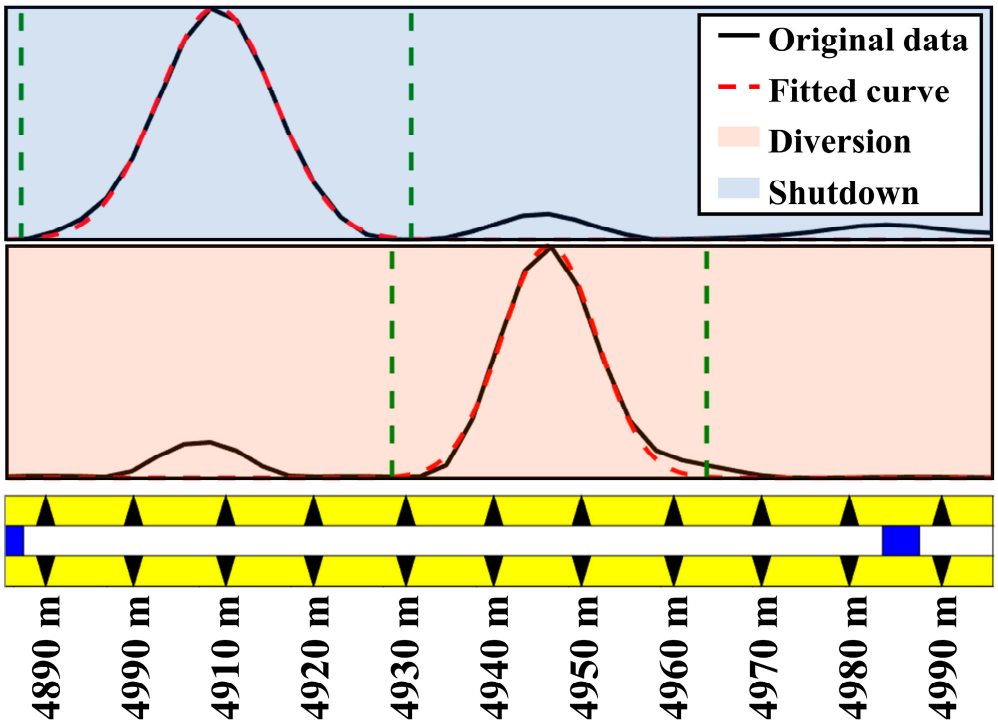


Figure 5. Reflection depths of diversion and shutdown. The yellow scale is the perforation position (m). The blue square are dissolvable bridge plugs.

2.3. Treating Pressure Response

Monitoring the pressure response during diversion using a treating pressure curve analysis is a common method for evaluating the diversion effectiveness. The fluid injection causes the fractures to gradually expand, with the treating pressure fluctuating with the fracture extension and complexity. When a diverter is introduced into the fracture, the successful diversion results in a significant increase in the treating pressure. A notable rise in the treating pressure indicates an effective diversion performance by the diverter, which forces the fracturing fluid to redistribute, potentially forming new fractures in a different direction or extending existing ones. Therefore, the magnitude of the treating pressure increase makes it possible to evaluate the diversion performance (see Figure 6). During the diverter injection, if the diverter effectively works, the diversion pressure rises rapidly and reaches a pressure spike, which is usually called a diversion pressure spike. The diversion pressure spike is used to evaluate the diversion performance (see Figure 6).

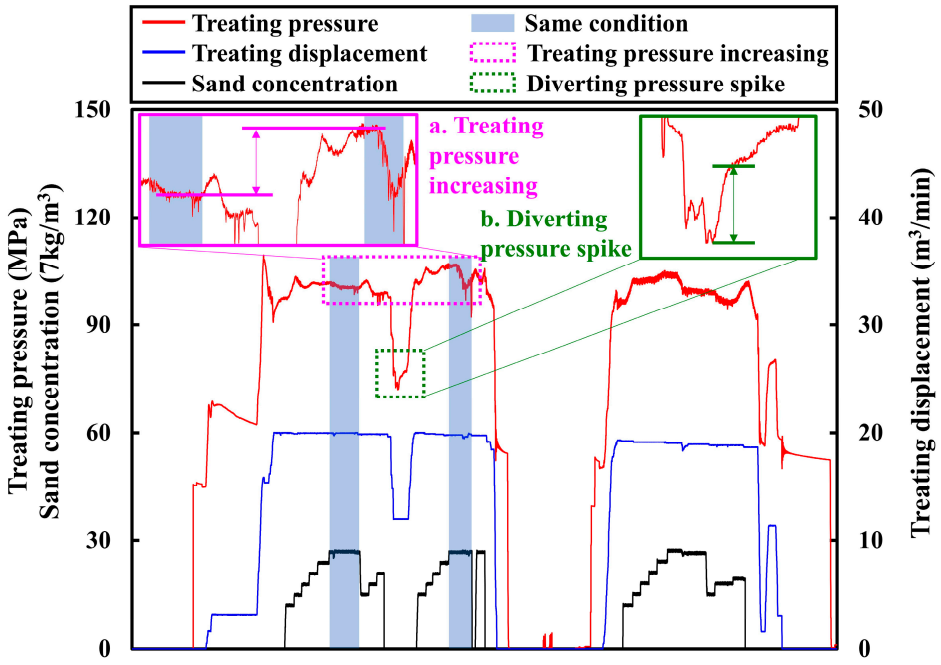


Figure 6. Treating pressure curve and the schematic diagram of the treating pressure increasing and the diverting pressure spike.

3. Field Data Results and Discussion

3.1. Well Introduction

The on-site test for evaluating the diversion performance was carried out in two shale gas horizontal wells on the same platform in Sichuan. The details of the well condition and treating scheme are listed in Table 1. Zipper fracturing and the bridge-perforation completion method were used in both wells. The depth of well 1 is 6168 m, with a horizontal segment length of 2700 m. The diversion plan for well 1 comprises 32 stages, among which 2 stages did not undergo diversion, 21 stages underwent single-time diversion, and 9 stages underwent dual-time diversion. A conic diverter was applied in well 1. The depth of well 2 is 6396 m, with a horizontal segment length of 2706 m. The diversion plan for well 2 consisted of 31 stages, among which 1 stage did not undergo diversion, 19 stages underwent single-time diversion, and 11 stages underwent dual-time diversion. A spherical and powdered diverter was utilized in well 2. Similar reservoir and rock properties, well structures, and diversion treating modes were manifested in well 1 and well 2, which can reduce the influence of irrelevant variables. The conic diverter and spherical and powdered diverter in the two wells were employed to analyze the influence of the diverter type on the diversion effectiveness. Single diversion and dual diversion were employed in each well independently to analyze the influence of diversion times on the diversion effectiveness.

Table 1. Details of well condition and treating scheme.

Well Number	Well 1	Well 2
Reservoir type	Shale	
The method of hydraulic fracturing	Diversion fracturing and staged fracturing	
The method of fracturing diagnosis	Water hammer diagnostics	
The method of treating	Zipper fracturing	
Depth of well	6168 m	6396 m
Horizontal segment length	2700 m	2706 m
Diversion plan stages	32	31
No diversion	2	1
Single-time diversion	21	19
Dual-time diversion	9	11
Diverter	Conic diverter	Spherical and powdered diverter

3.2. Results and Discussion

This section delves into the correlation between the water hammer oscillation time and diversion effectiveness from two aspects: (1) the association between the water hammer oscillation time and the probability of diversion calculated using the cepstrum analysis and error function; (2) the connection between the water hammer oscillation time and the treating pressure response obtained using a treating pressure curve analysis.

Firstly, the water hammer oscillation time dataset was quantified using the feature extraction method for oscillation times (Equations (1)–(4)), as shown in Figure 7a. The average oscillation times of well 1 and well 2 were 17.19 and 18.35, respectively. The oscillation time ranged from 2 to 27 in well 1 and from 2 to 28 in well 2. The 95% confidence intervals of the dataset mean, estimated using the normal distribution hypothesis [28], were [14.81, 19.56] and [15.92, 20.79], respectively. Secondly, the probability of diversion was calculated using the cepstrum analysis and error function (Equations (5)–(9)) as shown in Figure 7b. The average probabilities of diversion for well 1 and well 2 were 0.43 and 0.45, respectively. The 95% confidence intervals for the dataset means, estimated using the normal distribution hypothesis, were [0.33, 0.53] for well 1 and [0.34, 0.56] for well 2, respectively. Thirdly, the increases in the treating pressure and diversion pressure spikes were calculated using the treating pressure curve analysis (see Figure 7c,d). The average increases in the treating pressure for well 1 and well 2 were 2.21 and 1.71, respectively. The 95% confidence intervals for the dataset means, estimated using the normal distribution hypothesis, were [0.97, 3.45] for well 1 and [0.92, 2.45] for well 2, respectively. The average increases in the diversion pressure spikes for well 1 and well 2 were 1.37 and 0.87, respectively. The 95% confidence intervals for the dataset means, estimated using the normal distribution hypothesis, were [0.32, 2.41] for well 1 and [0.43, 1.30] for well 2, respectively. The results indicated that the average probability of diversion of well 1 and well 2 was similar, whereas the increases in the treating pressure and diversion pressure spikes of well 1 were higher than those of well 2. This discrepancy may be attributed to the conic diverter's superior effectiveness compared to the spherical and powdered diverter, resulting in a more effective diversion performance in well 1.

The water hammer oscillation times are plotted on the x-axis, with the corresponding probability of diversion on the y-axis. The relationship between the water hammer oscillation time and the probability of diversion is illustrated in Figure 8. The results indicate a negative correlation between the water hammer oscillation times and the probability of diversion; that is, lower oscillation times correspond to a higher probability of diversion. The fitting curves for the oscillation time versus the probability of diversion were determined to be $y_1 = -0.029x + 0.934$ and $y_2 = -0.0353x + 1.139$. The upper limit of the 95% confidence interval for the mean value of the dataset was calculated using the normal distribution hypothesis, as shown in the yellow area in Figure 8, while values below the 95% confidence level are represented in the blue area. The results indicate that when the oscillation time is greater than 20.79, the upper limit of the 95% confidence interval for the mean value of the dataset is reached, and the points are more likely to fall in the yellow area, indicating a higher probability of diversion. On the contrary, when the oscillation times is less than 20.79, the points are more likely to fall in the blue area, indicating a lower probability of diversion. Additionally, fewer oscillation times correspond to a higher probability of diversion. This may be due to changes in the main fluid acceptance zone between pre- and post-diversion.

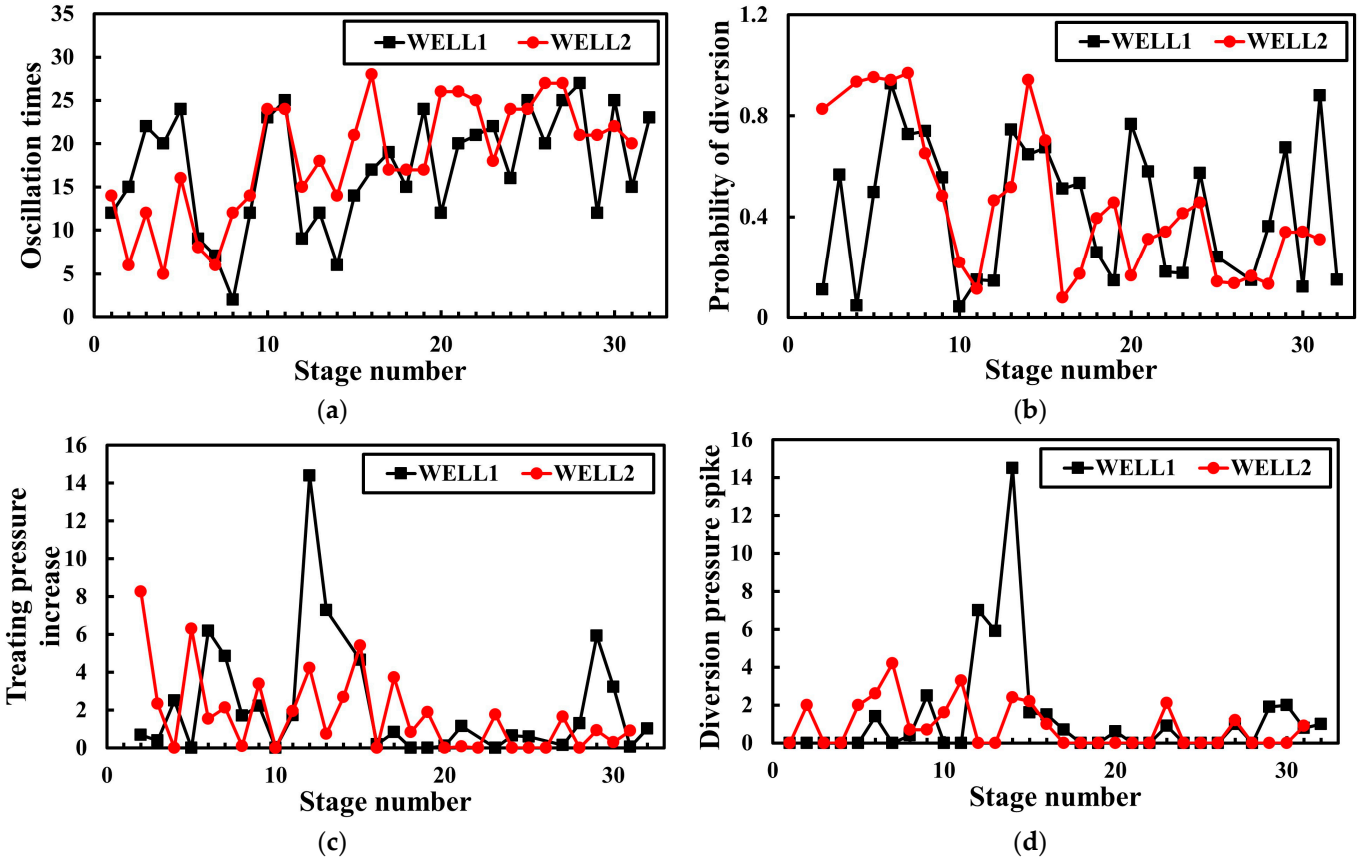


Figure 7. The results statistics of well 1 and well 2: (**a**) the water hammer oscillation time dataset; (**b**) the probability of diversion using cepstrum analysis and error function; (**c**) the treating pressure increasing; (**d**) the diversion pressure spike.

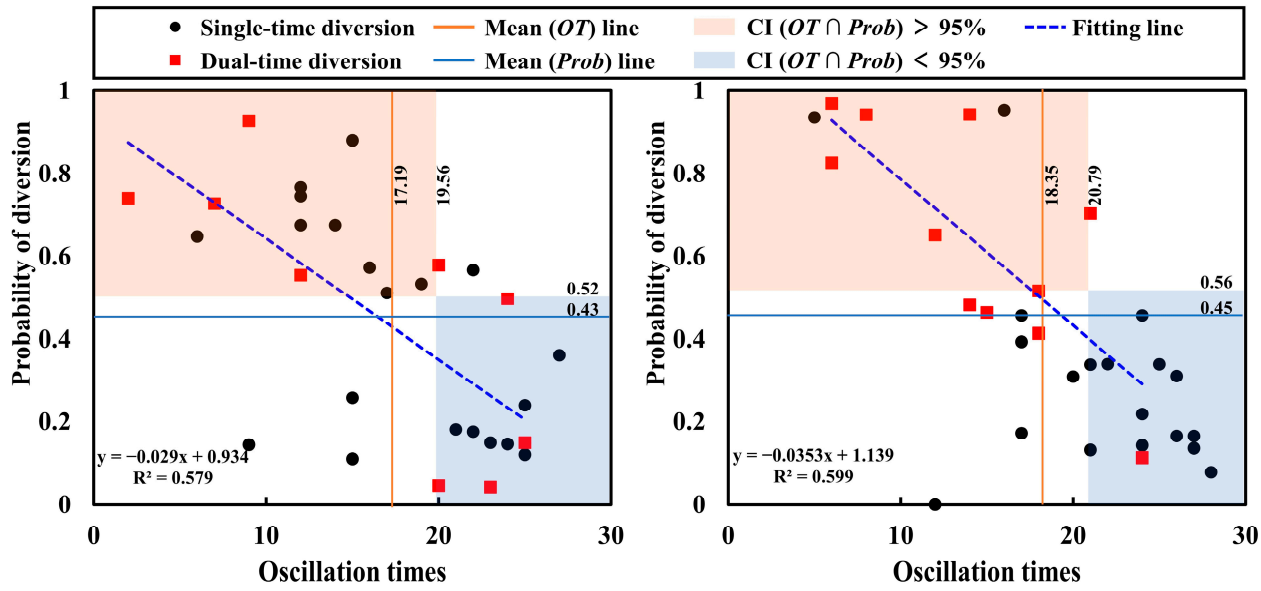


Figure 8. The relationship between the oscillation time and the probability of diversion from the cepstrum analysis and error function in well 1 and well 2.

The water hammer oscillation times are plotted on the x-axis, with the corresponding treating pressure increases and diversion pressure spike on the y-axes, respectively. The relationship between the water hammer oscillation time and the treating pressure increase is shown in Figure 9a,b, while the relationship between the water hammer oscillation

time and diversion pressure spike is shown in Figure 9c,d. The results indicate a negative correlation between water hammer oscillation times and the treating pressure response; the lower the oscillation time is, the higher the treating pressure increase and diversion pressure spike are. The fitting curves of the oscillation time versus the treating pressure increase were calculated as $y_1 = 7.674e^{-0.0751x}$ and $y_2 = 4.86e^{-0.0596x}$, and the fitting curves of the oscillation time versus the diversion pressure spike were calculated as $y_1 = 2.838e^{-0.0592x}$ and $y_2 = 2.78e^{-0.0704x}$. The upper limit of the 95% confidence interval for the mean value of the oscillation time and treating pressure response is shown in the yellow area in Figure 9, while values below the 95% confidence level are represented in the blue area. The results indicate that when the oscillation time is greater than 20.79, the upper limit of the 95% confidence interval of the mean value of the dataset is reached, and the points are more likely to fall in the yellow area, indicating a higher treating pressure increase and diversion pressure spike, resulting in a more effective diversion performance. On the contrary, when the oscillation time is less than 20.79, the points are more likely to fall in the blue area, indicating a poorer diversion performance. In general, lower oscillation times correspond to higher magnitudes of treating pressure increase and diversion pressure spike, indicating a higher probability of effective diversion. This may be because the effective performance of the diverter increases the liquid flow resistance in the wellbore–fracture–reservoir, resulting in the treating pressure increasing and the diversion pressure rising rapidly and reaching a peak after diversion.

Additionally, it was observed in well 2 that the diversion performance of dual diversion was superior to that of single diversion, as evidenced by the higher probability of diversion, the higher treating pressure increase, and the higher diversion pressure spike. This may be attributed to the irregular size and shape of the spherical and powdered diverter, which can more effectively adapt to the fracture apertures of different sizes and shapes during diversion. Consequently, a stronger plugging effect and superposition effect are shown in dual diversion.

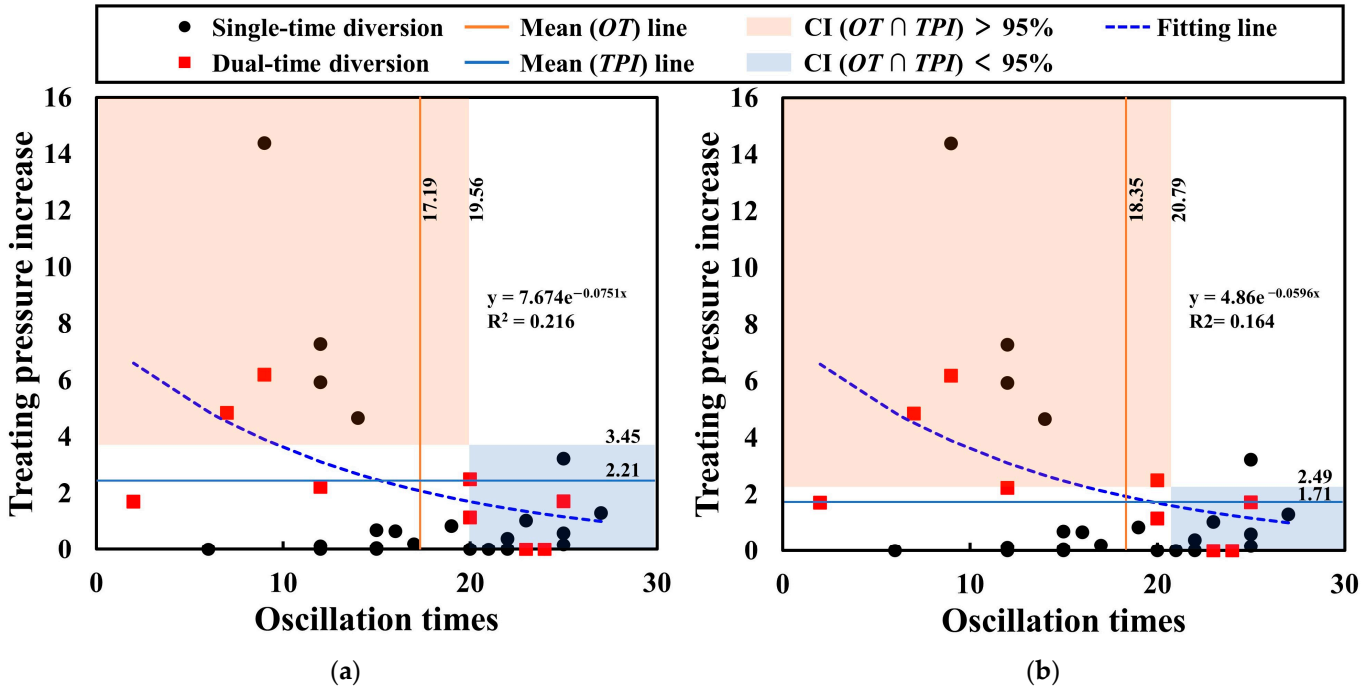


Figure 9. *Cont.*

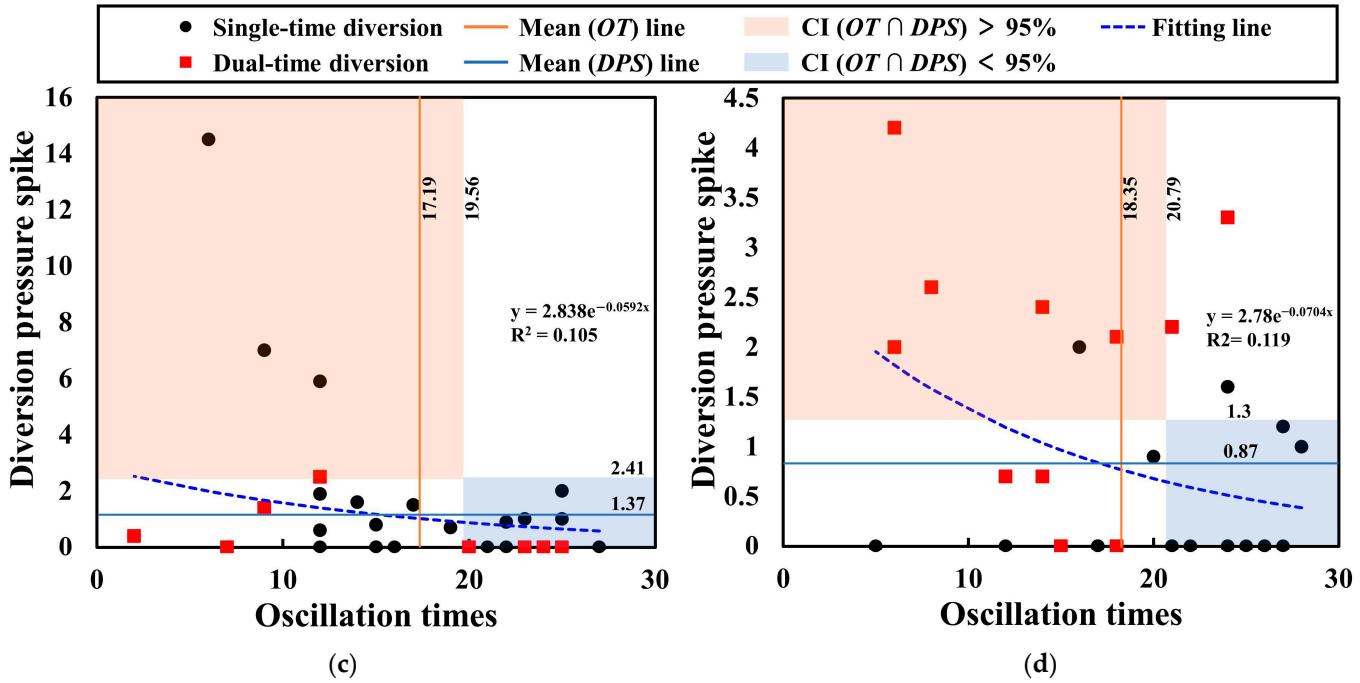


Figure 9. (1) The relationship between oscillation time and treating pressure increase in well 1 and well 2. (2) The relationship between oscillation time and diversion pressure spike.

A negative correlation was observed between the water hammer oscillation times and the diversion effectiveness in both wells. This is because more complex fractures lead to the increased friction in the wellbore–fracture–reservoir, indicating a greater energy absorption capacity in complex fractures, resulting in a greater attenuation of the water hammer signal. Therefore, a more effective diversion performance results in more complex fractures, leading to greater attenuation, presented as less water hammer oscillations.

3.3. A Rapid Judgment Method for Diversion Effectiveness Based on Oscillation Times

To analyze the relationship between the oscillation time and diversion effectiveness, a rapid judgment method for diversion effectiveness based on oscillation times was proposed in the shale reservoir. First, the feature extraction of the oscillation times is utilized in a field-sampled water hammer signal (Equations (1)–(4)). Second, the normal distribution hypothesis is used to calculate the 95% confidence interval of the mean value of the processed dataset. The upper limit of the confidence interval serves as a critical criterion for effectively evaluating the average oscillation time in a well.

$$\overline{N} = \frac{1}{n}\sum_{i=1}^{n} N_{P_i} \tag{10}$$

$$s = \sqrt{\frac{\sum_{i=1}^{n} \left(N_{P_i} - \overline{N}\right)^2}{n-1}} \tag{11}$$

Here, $\overline{x}$ is the average oscillation time of all stages, n is the number of stages, N_{P_i} is the oscillation time of the i-th stage, and s is the standard deviation of the dataset. We have obtained the critical condition (C) in the field cases.

$$C = \overline{N} + Z \times \frac{s}{\sqrt{n}} \tag{12}$$

Here, C is the upper limit of the 95% confidence interval of the mean value of the dataset, and Z is the critical value of the standard normal distribution. For 95% confidence,

$$Z \approx 1.96 \tag{13}$$

When the oscillation time is greater than the critical condition C, it is preliminarily determined that the diversion is effective at this stage. The probability of diversion effectiveness is as follows:

$$prob_{OT} = \frac{C - N_{P_i}}{C} \times 100\% \tag{14}$$

where $prob_{OT}$ is the probability of diversion effectiveness. This method can rapidly evaluate the probability of diversion effectiveness, being simple, intuitive, and field applicable.

4. Conclusions

The association between oscillation time and diversion effectiveness remains unclear in the current study. In this paper, the feature extraction method for water hammer oscillation times was proposed. Then, the correlation between the water hammer oscillation time and diversion effectiveness was clarified by taking the probability of diversion and the treating pressure response as the evaluation criteria. Finally, according to the analysis of the on-site test results, a rapid judgment method for diversion effectiveness based on the oscillation times was proposed.

The results indicated a negative correlation between the water hammer oscillation time and diversion effectiveness. Specifically, fewer oscillation times corresponded to a higher treating pressure increase, diversion pressure spike, and probability of diversion, indicating a higher likelihood of diversion effectiveness. This is attributed to lower oscillation times, representing higher friction and a greater energy absorption capacity in fractures, indicating a more complex fracture network.

The novel rapid judgment method for evaluating diversion effectiveness based on oscillation times was introduced for the first time. This method facilitates the rapid evaluation of the probability of diversion effectiveness, with its simplicity, intuitiveness, and applicability in the field. Nevertheless, further verification is required to ascertain its applicability in other lithological reservoirs.

Author Contributions: Conceptualization, B.L. and Y.W.; methodology, Y.Q. and P.Y.; software, Y.W.; validation, W.Y., Z.G. and R.W.; writing—original draft preparation, Y.W.; writing—review and editing, W.Y.; supervision, X.H. All authors have read and agreed to the published version of the manuscript.

Funding: This research received no external funding.

Data Availability Statement: Data are contained within the article. The original contributions presented in the study are included in the article; further inquiries can be directed to the corresponding author.

Conflicts of Interest: Authors Bingxiao Liu, Zhibin Gu, and Ran Wen are employed by Sichuan Changning Natural Gas Development Co., Ltd.; AuthorsBingxiao Liu and Zhibin Gu are employed by Sichuan Gemflower Xinsheng Oil and Gas Operation Service Co., Ltd.; Author Wenhan Yue is employed by PetroChina Southwest Oil and Gas Field Branch; The remaining authors declare that the research was conducted in the absence of any commercial or financial relationships that could be construed as potential conflicts of interest.

Nomenclature

P	w	Original water hammer signal
P'		Processed signal by mean normalization
P_{min}	MPa	The minimum value of the original water hammer signal
P_{max}	MPa	The maximum value of the original water hammer signal

$P_{min}{}'$		The minimum value of the processed water hammer signal
$P_{max}{}'$		The maximum value of the processed water hammer signal
T_{p2}, T_{p1}	s	The time corresponding to the two adjacent peaks
Period	s	The time required for the water hammer wave to complete a round trip in the wellbore
V_{pp}		The pressure difference between the peak and the valley
$\hat{x}(\tau)$		The cepstrum result of water hammer signal P
τ	s	The quefrency, with the characteristics of the reflection time dimension
t_i, t_j	s	Different physical times of intercepted water hammer signal
$V_{t_i,\tau}$, $V_{t_j,\tau}$		Vectors with different physical times
$F_{ij\tau}$		The scalar product of vectors with different physical times
F_τ		The function of the reflection time and energy magnitude
L	m	Location of the reflection event
a	m/s	Wave speed in the pipeline
σ	m	Location error
$\overline{N}$	time	The mean value of the oscillation times
n		The number of stages in a well
N_{P_i}	time	The oscillation time of the i-th stage
s		The standard deviation of the oscillation time dataset
C	time	The critical condition
Z		The critical value of the standard normal distribution
$prob_{OT}$	%	The probability of diversion effectiveness using the rapid judgment method for diversion effectiveness based on the oscillation times

References

1. Cao, X.; Wang, M.; Kang, J.; Wang, S.; Liang, Y. Fracturing Technologies of Deep Shale Gas Horizontal Wells in the Weirong Block, Southern Sichuan Basin. *Nat. Gas Ind. B* **2020**, *7*, 64–70. [CrossRef]
2. Al-Shargabi, M.; Davoodi, S.; Wood, D.A.; Ali, M.; Rukavishnikov, V.S.; Minaev, K.M. A Critical Review of Self-Diverting Acid Treatings Applied to Carbonate Oil and Gas Reservoirs. *Petrol. Sci.* **2023**, *20*, 922–950. [CrossRef]
3. Borisenko, A.; Parkhonyuk, S.; Zotov, K.; Korkin, R.; Kiselev, N.V.; Laptev, A.; Rapeyko, V.T. Advanced Pressure Monitoring Technique—New Horizons of Workover in Russia. In Proceedings of the SPE Russian Petroleum Technology Conference, Virtual, 11–13 October 2020. [CrossRef]
4. Kabannik, A.; Parkhonyuk, S.; Korkin, R.; Litvinets, F.; Dunaeva, A.; Nikolaev, M.; Usoltsev, D. Can We Trust the Diversion Pressure as a Decision-Making Tool: Novel Technique Reveals the Truth. In Proceedings of the Abu Dhabi International Petroleum Exhibition & Conference, Abu Dhabi, United Arab Emirates, 4–7 November 2018. [CrossRef]
5. Zhou, F.; Yuan, L.; Liu, X.; Wang, B.; Li, M.; Li, B. Advances and Key Techniques of Temporary Plugging and Diverting Fracturing. *Pet. Sci. Bull.* **2022**, *3*, 365–381. [CrossRef]
6. Sheng, M.; Zhang, J.; Zhang, Y.; Cheng, G.S. A New Data-Driven Effectiveness Evaluation Model of Temporary Plugging Fracturing for Horizontal Wells. *Nat. Gas Ind.* **2023**, *43*, 132–140.
7. Chen, H.; Gao, C.; Cai, C.; Sun, H. The Effectiveness and Influencing Factors of Blocking Perforation of Ball-Activated Temporary Plugging Fracturing in Horizontal Well. *Drill. Prod. Technol.* **2023**, *46*, 78–84.
8. Wang, B.; Zhou, F.; Yang, C.; Wang, D.; Yang, K.; Liang, T. Experimental Study on Injection Pressure Response and Fracture Geometry during Temporary Plugging and Diverting Fracturing. *SPE J.* **2020**, *25*, 573–586. [CrossRef]
9. Gomaa, A.M.; Nino-Penaloza, A.; McCartney, E.; Mayor, J. Engineering Solid Particulate Diverter to Control Fracture Complexity: Experimental Study. In Proceedings of the SPE Hydraulic Fracturing Technology Conference, The Woodlands, TX, USA, 9–11 February 2016. [CrossRef]
10. Bogdan, A.V.; Keilers, A.; Oussoltsev, D.; Lecerf, B. Real-Time Interpretation of Leak Isolation with Degradable Diverter Using High Frequency Pressure Monitoring. In Proceedings of the SPE Asia Pacific Oil & Gas Conference and Exhibition, Perth, Australia, 25–27 October 2016. [CrossRef]
11. Rodionov, Y.; Defeu, C.; Gakhar, K.; Mullen, K.; Mayo, J.T.; Shan, D.; Usoltsev, D.; Ejofodomi, E. Optimization of Infill Well Development Using a Novel Far-Field Diversion Technique in the Eagle Ford Shale. In Proceedings of the SPE/AAPG/SEG Unconventional Resources Technology Conference, Austin, TX, USA, 24–26 July 2017. [CrossRef]
12. Holzhausen, G.R.; Gooch, R.P. Impedance of Hydraulic Fractures: Its Measurement and Use for Estimating Fracture Closure Pressure and Dimensions. In Proceedings of the SPE/DOE Low Permeability Gas Reservoirs Symposium, Denver, CO, USA, 19–22 May 1985. [CrossRef]
13. Wang, X.; Hovem, K.; Moos, D.; Quan, Y. Water Hammer Effects on Water Injection Well Performance and Longevity. In Proceedings of the SPE International Symposium and Exhibition on Formation Damage Control, Lafayette, LA, USA, 13–15 February 2008. [CrossRef]

14. Urbanowicz, K.; Jing, H.; Bergant, A.; Stosiak, M.; Lubecki, M. Progress in Analytical Modeling of Water Hammer. *ASME J. Fluids Eng.* **2023**, *145*, 081203. [CrossRef]
15. Parkhonyuk, S.; Fedorov, A.; Kabannik, A.; Korkin, R.; Nikolaev, M.; Tsygulev, I. Measurements While Fracturing: Nonintrusive Method of Hydraulic Fracturing Monitoring. In Proceedings of the SPE Hydraulic Fracturing Technology Conference and Exhibition, The Woodlands, TX, USA, 23–25 January 2018. [CrossRef]
16. Korkin, R.; Parkhonyuk, S.; Fedorov, A.; Badazhkov, D.; Kabannik, A. High Frequency Pressure Monitoring and Data Analytics for Stimulation Efficiency Determination: New Perspectives or Potential Limits. In Proceedings of the SPE Hydraulic Fracturing Technology Conference and Exhibition, The Woodlands, TX, USA, 4–6 February 2020. [CrossRef]
17. Parkhonyuk, S.; Korkin, R.; Kabannik, A.; Fedorov, A.; Nikolaev, M.; Litvinets, F. Novel Monitoring Technology Helps to Make Informed Decisions and Maximize the Efficiency of Completion Strategy. In Proceedings of the SPE/AAPG/SEG Unconventional Resources Technology Conference, Houston, TX, USA, 23–25 July 2018. [CrossRef]
18. Ciezobka, J.; Maity, D.; Salehi, I. Variable Pump Rate Fracturing Leads to Improved Production in the Marcellus Shale. In Proceedings of the SPE Hydraulic Fracturing Technology Conference, The Woodlands, TX, USA, 9–11 February 2016. [CrossRef]
19. Iriarte, J.; Merritt, J.; Kreyche, B. Using Water Hammer Characteristics as a Fracture Treating Diagnostic. In Proceedings of the SPE Oklahoma City Oil and Gas Symposium, Oklahoma City, OK, USA, 27–31 March 2017. [CrossRef]
20. Hu, X.; Luo, Y.; Zhou, F.; Qiu, Y.; Li, Z.; Li, Y. Evaluation of Multi-Fractures Geometry Based on Water Hammer Signals: A New Comprehensive Model and Field Application. *J. Hydrol.* **2022**, *612*, 128240. [CrossRef]
21. Luo, Y.; Hu, X.; Zhou, F.; Qiu, Y.; Lu, X.; Li, J.; Wang, Y. A New Water Hammer Decay Model: Analyzing the Interference of Multiple Fractures and Perforations on Decay Rate. *SPE J.* **2023**, *28*, 1973–1985. [CrossRef]
22. Panjaitan, M.L.; Moriyama, A.; McMillan, D.; Dunaeva, A.; Rutledge, L.; Xu, J.; Parkhonyuk, S.; Kabannik, A.; Korkin, R.; Warren, M.; et al. Qualifying Diversion in Multi Clusters Horizontal Well Hydraulic Fracturing in Haynesville Shale Using Water Hammer Analysis, Step-Down Test and Microseismic Data. In Proceedings of the SPE Hydraulic Fracturing Technology Conference and Exhibition, The Woodlands, TX, USA, 23–25 January 2018. [CrossRef]
23. Chang, H.; Yi, D.Q.; Lv, Y.; Zhao, M.; Cao, P.L.; Zhang, L.; Hou, R.; Di, Y.L.; Chen, J.; Zhang, L.; et al. Outside the Box: Innovative Application of Diversion as a Replacement for Bridge Plug. In Proceedings of the SPE Middle East Oil & Gas Show and Conference, Event Canceled, 15 November 2021. [CrossRef]
24. Alobaid, H.; Khan, A.M.; Almulhim, A.; Hansen, J.; Kabannik, A. Comprehensive Design and Diagnostic Approach for Horizontal Completions in Carbonate Environment. In Proceedings of the ADIPEC, Abu Dhabi, United Arab Emirates, 31 October 2022. [CrossRef]
25. Alobaid, H.; Khan, A.M.; Hansen, J.; Khudorozhkova, A. Stimulation Efficiency with Significantly Fewer Stages: Perforation Strategy Combined with Multimodal Diverters and Novel Nonintrusive Monitoring Algorithm. In Proceedings of the SPE Annual Technical Conference and Exhibition, Houston, TX, USA, 3–5 October 2022. [CrossRef]
26. Haustveit, K.; Dahlgren, K.; Greenwood, H.; Peryam, T.; Kennedy, B.; Dawson, M. New Age Fracture Mapping Diagnostic Tools-A STACK Case Study. In Proceedings of the SPE Hydraulic Fracturing Technology Conference and Exhibition, The Woodlands, TX, USA, 25 January 2017. [CrossRef]
27. Qiu, Y.; Hu, X.; Zhou, F.; Li, Z.; Li, Y.; Luo, Y. Water Hammer Response Characteristics of Wellbore-Fracture System: Multi-Dimensional Analysis in Time, Frequency and Quefrency Domain. *J. Pet. Sci. Eng.* **2022**, *213*, 110425. [CrossRef]
28. Montgomery, D.C.; Runger, G.C.; Hubele, N.F. *Engineering Statistics*; John Wiley & Sons: Hoboken, NJ, USA, 2009.

Disclaimer/Publisher's Note: The statements, opinions and data contained in all publications are solely those of the individual author(s) and contributor(s) and not of MDPI and/or the editor(s). MDPI and/or the editor(s) disclaim responsibility for any injury to people or property resulting from any ideas, methods, instructions or products referred to in the content.